

Comparison of Calculated and Measured Flicker Values for Two Different Network Topologies

Miloš Maksić, *Student Member, IEEE*, Boštjan Blažič, *Member, IEEE* and Igor Papič, *Senior Member, IEEE*

Abstract — Frequent customer complaints resulting from high flicker levels in part of the Slovenian high-voltage network have necessitated an in-depth study of the source of such high flicker levels and means of flicker mitigation. Flicker measurements in several network nodes point to a local arc furnace as the single largest source of high flicker in the area. Calculation of flicker levels in the area via load flow and current injection method for two different network topologies – with connected and disconnected 110 kV busbars near the arc furnace – prove to be in good agreement with measurements. The current injection method is further employed in two simulation cases of flicker propagation in the network in 2020 and in an additional simulation, performed after the assumed installation of a STATCOM device.

Index Terms—Flicker, power quality, flicker measurements, load-flow based method, current injection method, flicker mitigation, STATCOM.

I. INTRODUCTION

FREQUENT customer complaints have shown that voltage flicker represents by far the largest power quality problem in part of the Slovenian power network. Several studies [1,2] have pointed to a local arc furnace as the single largest source of high flicker in the area. Its intermittent and highly irregular consumption of active and reactive power causes voltage fluctuations in the network. These fluctuations propagate from the arc furnace throughout the high voltage (HV) network and then to the medium-voltage (MV) and low-voltage (LV) grids where they cause considerable problems associated with the varying luminosity of lamps. Depending on the intensity of these variations, humans can experience these variations as an annoying flicker sensation. Flicker is one of 13 power quality indices described in the widely accepted EN 50160 power quality standard [3]. Another standard IEC/TR 61000-3-7 [4] provides detailed assessment of flicker limits at different voltage levels.

The first step in solving flicker problems in the area is the development of suitable methods to assess flicker levels in the network without the need for measurements. Such methods

become even more practical when studying how future network reinforcements or other flicker mitigation techniques, e.g. the installation of SVC and STATCOM devices, affect damping of flicker [5]-[10].

Two such methods for evaluating flicker propagation in the network are used in the paper – load-flow based method and current injection method [5]. The accuracy of both methods is verified with measurements of flicker levels in several nodes throughout the network for two different network topologies – with connected and disconnected local 110 kV busbars, which greatly affects flicker propagation.

One of these methods is further used in simulation of flicker propagation in three cases. The first case reveals that higher network short-circuit power in 2020, resulting from various line reinforcements and new generating units, will not solve flicker problems in the area. In the second case, an extended 400 kV line to the arc furnace is studied. Flicker levels fall throughout the area, yet this solution is impractical from an economic and other standpoints. Therefore the installation of a STATCOM device, as studied in the third case, is determined as the only viable method for solving power quality problems in the area.

II. FLICKER AND FLICKER PROPAGATION IN POWER NETWORKS

A. Definition of flicker

Flicker can be described as an annoying visual sensation of light flickering caused by the variation of illumination intensity of light sources. As this variation is often caused by voltage fluctuations, i.e. fluctuations of voltage rms values in the network, this problem is often denoted as voltage flicker.

References [3] and [4] cite two indexes for determining flicker levels in the network: short-term flicker severity index P_{st} and long-term flicker severity index P_{lt} . P_{st} is based on statistical evaluation of ten-minute intervals of instantaneous flicker perception $S(t)$ that presents one of the outputs of the flickermeter [3]. P_{lt} is based on an evaluation of twelve successive P_{st} values. In areas that fall under the influence of a large source of flicker with longer operating periods, such as the arc furnace, the use of index P_{lt} is encouraged.

EN 50160 sets $P_{lt} = 1$ as the permissible flicker level in medium-voltage nodes which should not be exceeded in 95 % of the weekly measurement time. The standard makes no reference to permissible flicker levels in HV systems. Even though the flicker transfer factor from HV to MV networks is substantially smaller than 1 (~ 0.8), the same level $P_{lt} = 1$ is

This work was supported by Milan Vidmar Electric Power Research Institute - EIMV under Grant S-1167.

M. Maksić is with Faculty of electrical engineering, University of Ljubljana, Ljubljana, Slovenia (e-mail: milos.maksic@fe.uni-lj.si).

B. Blažič is with the Faculty of Electrical Engineering, University of Ljubljana, Ljubljana, Slovenia (e-mail: bostjan.blazic@fe.uni-lj.si).

I. Papič is with Faculty of electrical engineering, University of Ljubljana, Ljubljana, Slovenia (e-mail: igor.papic@fe.uni-lj.si).

often used for HV networks since it provides enough protection and reserve from all other intermittent loads, acting in MV and LV levels which also contribute to overall flicker.

B. Flicker propagation in a network

Flicker is caused by fluctuations of voltage rms values $\Delta|V|$. A simple method to evaluate flicker propagation is thus the use of voltage transfer coefficients, which can be denoted as the ratio of relative voltage changes in two nodes "i" and "j":

$$kv_{i,j} = \frac{\Delta v_i}{\Delta v_j} \quad (1)$$

Flicker transfer coefficients $kp_{i,j}$ can be similarly defined as the ratio of P_{lt} in both nodes. In special cases of frequency independent loads both $kp_{i,j}$ and $kv_{i,j}$ are the same and therefore flicker in node "i" is:

$$P_{lt,i} = P_{lt,j} \cdot kp_{i,j} = P_{lt,j} \cdot kv_{i,j}. \quad (2)$$

Coefficients $kp_{i,j}$ depend on the network topology, power generation and load consumption. Higher short-circuit power results in smaller relative voltage changes and thus smaller flicker.

Obtaining coefficients (1) in radial networks is fairly simple and straightforward [5,6]. Fig. 1 shows a simple radial network. Flicker propagating from a downstream fluctuating source in node C to a voltage source of higher short-circuit power in node A is attenuated according to the impedances:

$$kv_{C,A} = \left| \frac{Z_A}{Z_A + Z_{A-C}} \right| = \left| \frac{Z_{src}}{Z_{src} + Z_{L1} + Z_{TR1}} \right|. \quad (3)$$

Z_{src} is the voltage source impedance, Z_{L1} is the impedance of the lines and Z_{TR1} the transformer impedance.

In the opposite case of upstream to downstream flicker transfer from node A to node B in Fig. 1, flicker mostly remains unchanged and $kv_{A,B} \approx 1$. Flicker does attenuate somewhat though when propagating through the transformers.

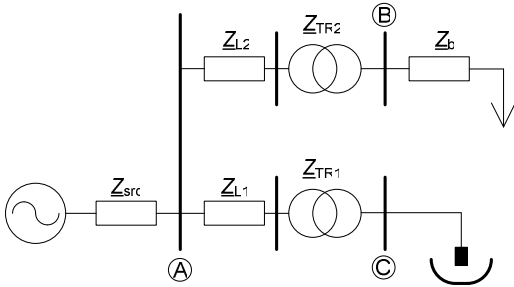


Fig. 1: A simple radial system.

These methods however become impractical for much larger meshed networks. In this case both time-dependent [1] and stationary [5] analyses can be employed. Both can yield results that are in good compliance with the measurements. This paper will focus on two methods for obtaining $kp_{i,j}$ with stationary analyses – load-flow based method and current injection method [5].

C. Load-flow based method

A part of the network under study is shown in Fig. 2. Node

A can be assumed as the point of common coupling of the arc furnace with the rest of the network.

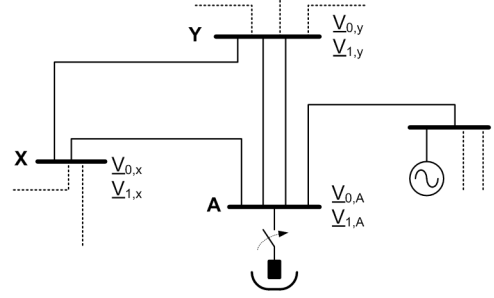


Fig. 2: Voltage phasors before (0) and after (1) load switching.

Relative voltage change in node X can be calculated according to:

$$\Delta v_x = \frac{\Delta V_x}{V_x} = \frac{|V_{0,x}| - |V_{1,x}|}{\frac{|V_{0,x}| + |V_{1,x}|}{2}} \quad (4)$$

$V_{0,x}$ represents voltage phasor in node X with disconnected load in node A, and $V_{1,x}$ represents voltage phasor in node X with connected load in node A. Relative voltage changes in all the network nodes can thus be obtained with two load-flow calculations with and without the load in node A. The next step requires calculation of coefficients (1) and lastly of flicker values (2) from a single or multiple flicker reference.

Voltage changes in nodes with high short-circuit power will be sufficiently small and flicker will be accordingly attenuated. Flicker is also greatly attenuated when propagating through transformers from LV and MV to HV levels. In principle, only the location of the disturbing load A and not its size matter, since relative voltage changes should be equal for switching of any load power. Yet considering various nonlinearities in the network, choosing a load approximately equal to the normal consumption of the arc furnace should be sufficient [1,2].

D. Current injection method

Disturbing load in node A in Fig. 2 is replaced with a current source injecting a three-phase current I_A into the rest of the system. The current will propagate from node A throughout the network and will cause voltage drops in nodes according to the impedances of loads and network elements. For a system with N nodes we can write:

$$\begin{bmatrix} 0 \\ \vdots \\ 0 \\ I_A \\ 0 \\ \vdots \\ 0 \end{bmatrix} = \underbrace{\begin{bmatrix} Y_{11} & \cdot & \cdot & \cdot & \cdot & \cdot & Y_{1N} \\ \cdot & \cdot & \cdot & \cdot & \cdot & \cdot & \cdot \\ \cdot & \cdot & \cdot & \cdot & \cdot & \cdot & \cdot \\ \cdot & \cdot & \cdot & Y_{AA} & \cdot & \cdot & \cdot \\ \cdot & \cdot & \cdot & \cdot & \cdot & \cdot & \cdot \\ \cdot & \cdot & \cdot & \cdot & \cdot & \cdot & \cdot \\ Y_{N1} & \cdot & \cdot & \cdot & \cdot & \cdot & Y_{NN} \end{bmatrix}}_{\text{system admittance matrix } Y} \cdot \begin{bmatrix} V_1 \\ V_2 \\ \vdots \\ V_A \\ \vdots \\ V_{N-1} \\ V_N \end{bmatrix} \quad (5)$$

Y_{ij} represents the negative value of admittance between nodes "i" and "j" and Y_{ii} represents the sum of admittances connected to node "i". Voltage phasors on the right side of (5) can be acquired by solving $V=Y^{-1}I$ or by computer simulation. Calculating relative voltage changes for (1) is not necessary

since all voltages can be referenced with the same randomly chosen voltage U_0 . Equation (1) can thus simply be written as:

$$kV_{ij} = \frac{|V_i|}{|V_j|}. \quad (6)$$

Generators are modeled with their subtransient/transient impedances and, depending on the computational program, P - Q loads can be replaced with a R - L combination.

III. FLICKER MEASUREMENTS FOR TWO NETWORK TOPOLOGIES

A. Network under study

Fig. 3 shows 14 nodes where flicker measurements were carried out. The 100 MVA arc furnace transformer is connected to a 110 kV node 1. The short-circuit power in this and other 110 kV nodes is relatively small and therefore flicker propagates to these nodes with relatively small attenuation. Generators G1-G3 are smaller units (< 50 MVA) and do not significantly attenuate flicker levels in the area. Primary sources of higher short-circuit power in the area are a 120 MVA generator G4 and the 220 kV and 400 kV networks.

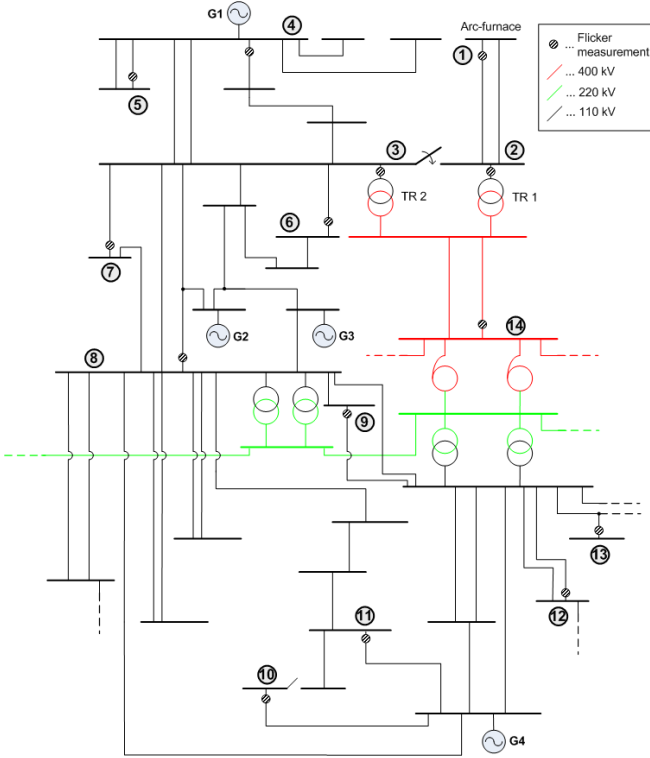


Fig. 3: Network under study.

Of special interest is a 400/110 kV transformer substation near the arc furnace where measurements were carried out for two different busbar operations:

- connected nodes 2 and 3,
- disconnected nodes 2 and 3.

Connected busbars result in parallel operation of two 300 MVA 400/110 kV transformers TR 1 and TR 2, both supplying the arc furnace and other nodes with power, while

disconnected busbars result in one transformer supplying the arc furnace and the other transformer supplying the remaining consumers. Both configurations significantly affect the short-circuit power in node 1 and have a great impact on flicker propagation.

B. Flicker measurements

Two weeks of field measurements for connected and disconnected busbars 2 and 3 were carried out in accordance with specifications in EN50160.

Fig. 4 shows P_{st} and P_{lt} values measured in node 1 with connected busbars. Rapid changes of both indexes mark intervals when the arc furnace stops or starts operation.

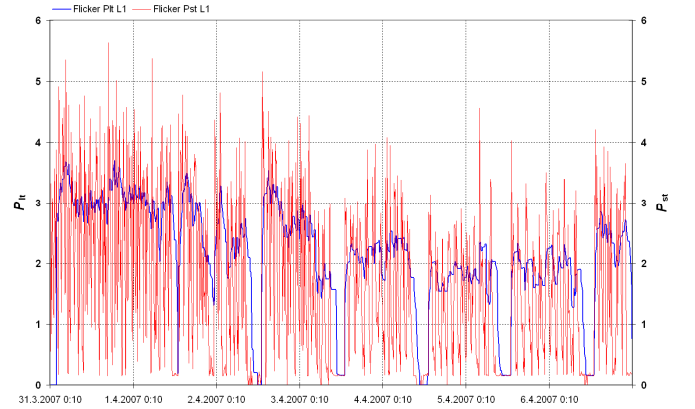


Fig. 4: Flicker P_{st} and P_{lt} (L1 110 kV node 1, connected busbars).

Fig. 5 shows P_{lt} values of flicker in several network nodes for connected busbars 2 and 3, and Fig. 6 shows P_{lt} levels for disconnected busbars. The shape of P_{lt} levels caused by the arc furnace (node 1) corresponds well with the shapes of measurements in other nodes shown in Fig. 5 and 6. Use of index P_{st} in Fig. 4 would make such comparisons much more difficult. P_{lt} levels are attenuated but still coincide in time when propagating throughout the area. This proves that the arc furnace is the only major source of flicker in the area.

Connected busbars in Fig. 3 result in high flicker levels throughout the area. The highest P_{lt} values are recorded in node 1 and are still close to the limit value $P_{lt} = 1$ in other 110 kV nodes. Flicker levels however diminish below the P_{lt} limit value in the area after transformer busbars 2 and 3 are separated. Obviously flicker greatly attenuates when it propagates through both transformers TR 1 and TR 2 and reaches the other 110 kV busbars. This occurs even though flicker levels in node 1 almost double compared to the operation with connected busbars due to smaller short-circuit power in this node.

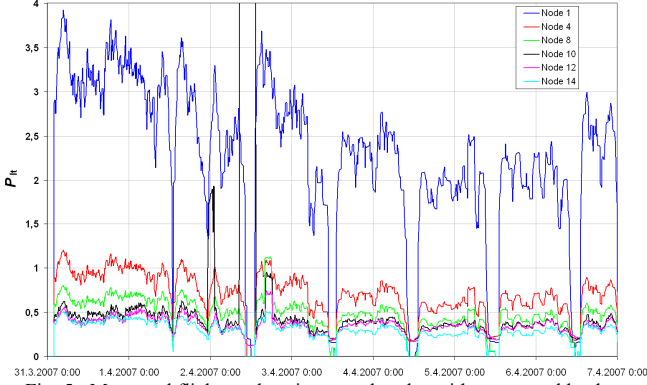


Fig. 5: Measured flicker values in several nodes with connected busbars.

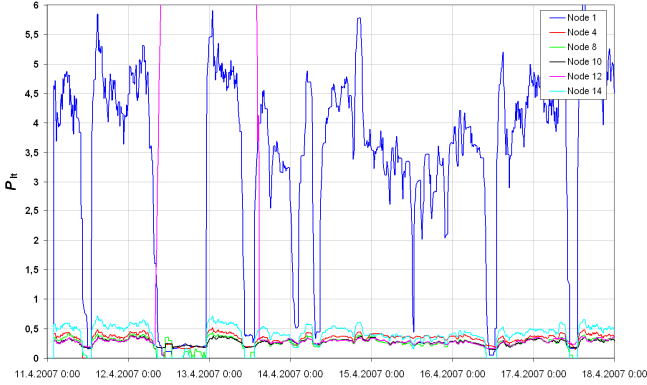


Fig. 6: Measured flicker values in several nodes with disconnected busbars.

In the next step, $P_{it,95\%}$ values of flicker are obtained according to EN50160. The values are shown in Table I.

TABLE I
OBTAINED VALUES OF $P_{IT,95\%}$ FOR BOTH MEASUREMENT WEEKS

Node	Connected busbar operation	Disconnected busbar operation
Node 1	3.44	5.31
Node 2	1.13	3.03
Node 3	1.13	0.47
Node 4	1.05	0.44
Node 5	1.05	0.44
Node 6	1.11	0.47
Node 7	0.93	0.47
Node 8	0.72	0.38
Node 9	0.70	0.41
Node 10	0.62	0.40
Node 11	0.66	0.42
Node 12	0.56	0.40
Node 13	0.51	0.49
Node 14	0.44	0.61

Table I shows that with connected busbar operation flicker levels exceed the limit value in 6 of 14 nodes and with disconnected operation in just 2 of 14 nodes.

Concerning power quality, the disconnected operation of busbars 2 and 3 is obviously the preferred choice since flicker levels in all the nodes fall even below the network planning level of flicker $P_{it} = 0.6$. Nevertheless this solution is not applicable in practice for many reasons. Firstly, the newer of both transformers, TR 2 was originally planned as a back-up

for the degraded and older TR 1. In the case of TR 1 failure, nodes 2 and 3 would have to be connected and power quality in the area would again deteriorate. There are also concerns regarding lower short-circuit power by the arc furnace, which can cause the melting process to become more unstable thus causing even higher flicker.

IV. SIMULATION OF FLICKER PROPAGATION

A. Comparison of both methods with measurements

Results of flicker propagation in the network shown in Fig. 3 for load-flow based and current injection method are further described. Both methods yield voltage transfer coefficients. A reference value of flicker is required in a single node. Since at this point we concentrate solely on comparison of simulated results with measurements, we can choose a measured value P_{it} in node 3 in Table I as a reference value for both cases of busbar operation. Value in node 1 could be chosen as well, but high measured flicker levels are often misleading because the power-quality meters determine correct flicker values only in a limited range.

Fig. 7 shows simulation results for both methods as well as measured P_{it} values for the case with connected busbars 2 and 3. In general, both methods are in good agreement with measured results. Somewhat large error in node 13 is an indication that this is a relatively distant node that comes under the influence of other sources of flicker. Results for node 1 are not shown in Fig. 7 since as mentioned before, measurements of such high flicker levels are prone to errors and would also make a graphical comparison of other nodes more difficult.

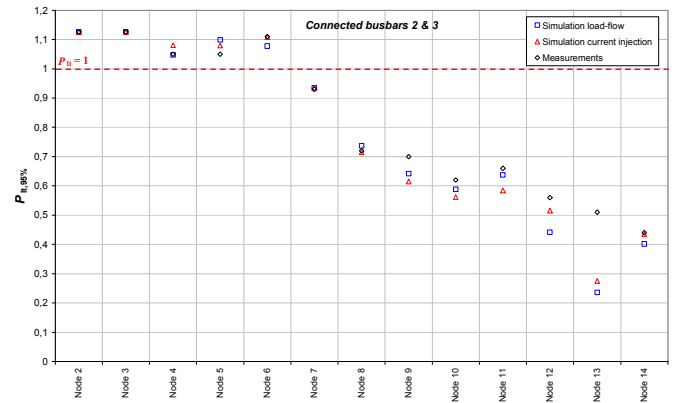


Fig. 7: Measured and calculated flicker values with connected busbars.

Fig. 8 similarly shows results with disconnected busbars. Both methods again provide good results when compared with measurements. Similarly to node 1, the results for node 2 are not presented since flicker values in this node reach high values.

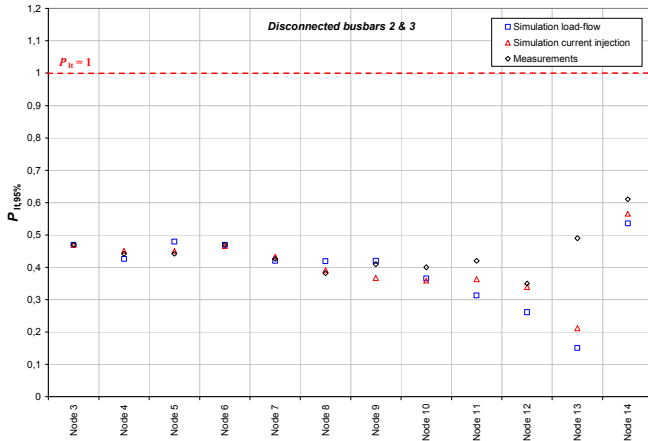


Fig. 8: Measured and calculated flicker values with disconnected busbars.

Fig. 9 shows the percentage error of both methods, which remains primarily below 10%. With node 13, the error is significant due to the other sources of flicker acting upon this node.

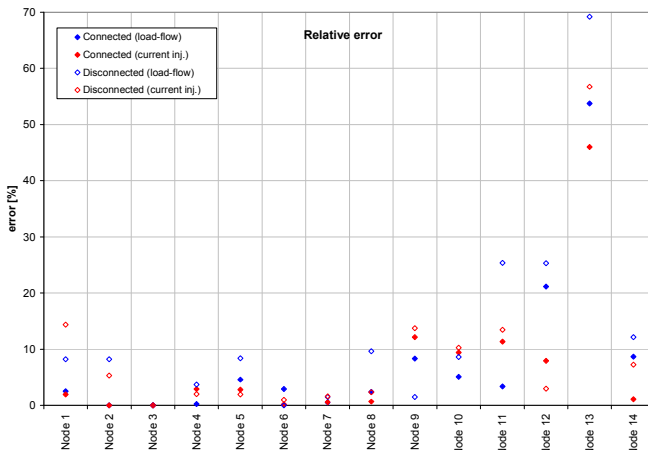


Fig. 9: Percentage errors of both methods compared to the measurements.

The accuracy of both methods varies in all 14 nodes, yet somewhat smaller errors are generally achieved with the current injection method (red marks in Fig. 9). Thus the current injection method will be further used in subsequent simulations of flicker propagation.

B. Simulation of flicker propagation in 2020

Various new generating units and network reinforcements on all HV levels are planned to be installed in the Slovenian power system by 2020. All changes in the network under study are shown in Fig. 10. The existing 120 MVA G4 generating unit will be upgraded to a capacity of 200 MVA. A new 100 MVA unit G5 shown in Fig. 10 is also planned to start operation. Fig. 10 additionally shows new nodes and lines in 2020. New nodes are marked with a red asterisk *. Another important aspect that will affect flicker in the area is the higher short-circuit power in 220 kV and 400 kV networks, due to new generating units in the Slovenian system not shown in Fig. 10. Short-circuit power in the 400 kV node 14 is currently estimated at 8,600 MVA with roughly 13,000 MVA estimated

for 2020. Since, as mentioned above, connected operation of nodes 2 and 3 is unacceptable, both nodes are merged into a single node 2.

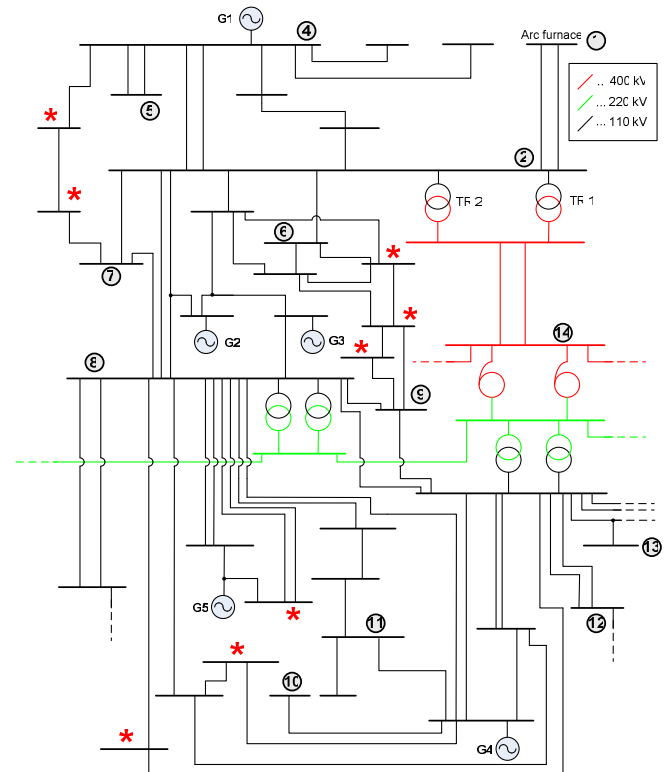


Fig. 10: Network under study in the year 2020.

The calculation of flicker propagation with the current injection method is repeated for the network in Fig. 10. There are several possibilities in choosing the flicker reference value. Ref. [11] points at the next approximate formula:

$$P_{st} = k_{st} \cdot \frac{S_{EAF}}{S_{SC}}, 45 < k_{st} < 85, \quad (7)$$

where P_{st} denotes the short-time flicker, S_{SC} the short-circuit power at the point of the connection of the arc furnace transformer to the network, S_{EAF} represents the rated power of the furnace transformer and factor k_{st} primarily depends on the type of the arc furnace.

Forming a simple ratio of P_{st} values from (7), we obtain:

$$\frac{P_{st1}}{P_{st2}} = \frac{S_{SC2}}{S_{SC1}} \approx \frac{P_{lt1}}{P_{lt2}}. \quad (8)$$

The above approximation for P_{lt} is valid only for the case of longer and more stable melting process in the arc furnace. A reference value of flicker P_{lt} for 2020 can thus be derived by using (8). Given that the short circuit power in node 1 increases from the present 1,400 MVA to approximately 1,500 MVA in 2020, the reference value $P_{lt} = 3.44$ in Table I is corrected to $P_{lt} = 3.21$ for 2020. Larger short-circuit power in the network alone thus does not significantly reduce flicker in this node.

Nevertheless, the above approximation of $P_{lt} = 3.21$ is not a particularly conservative estimate since it does not take into

account a potential larger production of the arc furnace in the steelworks and also presumes an unchanged melting process in the facility. These two factors could both further increase future flicker levels. Thus an estimate of $P_{it} = 3.44$ as in Table I will be used as a reference value in node 1 for 2020. This will also make a comparison of present and future flicker values in Table I easier.

Fig. 11 shows simulated results for 2020 compared to the simulated results from the current injection method in Fig. 7. A comparison of simulated results provides a better insight into flicker damping.

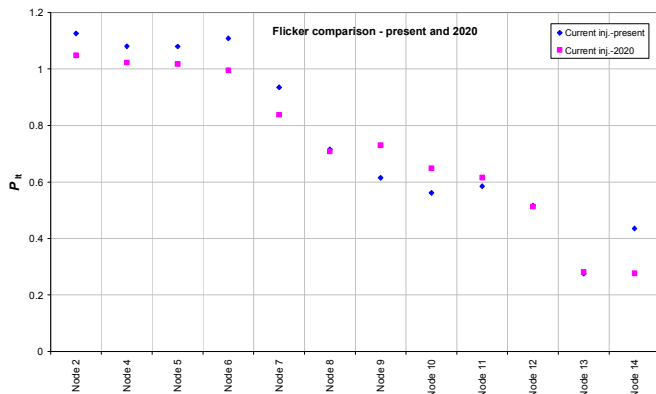


Fig. 11: Comparison of flicker values – present and in 2020 (both by current injection method).

Results for node 1 are again omitted. According to Fig. 11, larger short-circuit power in 2020 will attenuate flicker P_{it} levels in nodes 2-7 by approximately 0.1 value, yet in nodes 8-13 flicker levels will not only remain unchanged but will actually further increase. This can be attributed to several new tie lines connecting the arc furnace electrically closer to nodes 8-13 and enabling flicker to propagate even further. Greater capacity of generating unit G4, new unit G5 and larger short-circuit power in the area from the 400 kV and 220 kV networks will not significantly alleviate flicker levels in the area.

C. Simulation of flicker propagation with extended 400 kV line

A new 400 kV line extending from 110 kV node 2 directly to the arc furnace in node 1, as shown in Fig. 12, offers another possibility for damping high flicker levels in the area. This leaves other consumers on the 110 kV level connected to node 2 operating on a single 400/110 kV transformer.

The current injection method is again employed in the calculation of flicker propagation in the network. The network for 2020 from Fig. 10 is used, considering the change in Fig. 12.

Once again the same conservative estimate of flicker $P_{it} = 3.44$ in node 1 is used as a reference value. This is a highly unlikely value due to much larger short-circuit power provided by the 400 kV line. It will again make a comparison of this case easier.

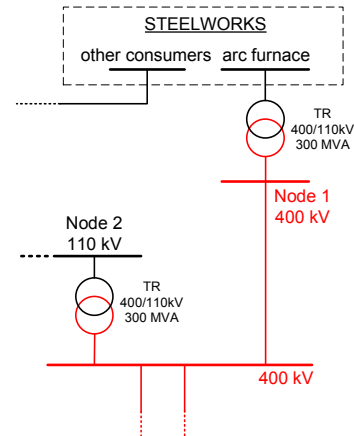


Fig. 12: New 400 kV line to the arc furnace.

The calculation results are shown in Fig. 13 and are compared with results for the year 2020 shown in Fig. 11.

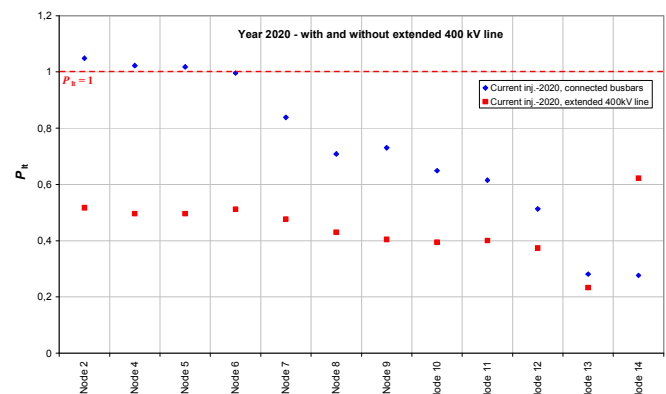


Fig. 13: Comparison of flicker values for the year 2020, with and without the extended 400 kV line (both by current injection method).

For the case of a new 400 kV line, flicker values across the network fall below 0.6, even though the estimated reference flicker in node 1 is relatively high. In reality we can expect these levels to fall below 0.5 or even 0.4. The advantage that the new line brings is clearly evident in Fig. 13.

The new 400 kV line has an additional advantage for the steelworks, since larger short-circuit power at the arc furnace improves the melting of iron. A new 400 kV line would however require a broader corridor than the existing two 110 kV lines on a single pylon. The placement of new lines involves lengthy processes of obtaining construction and installation permissions. This and other purely economic reasons make the placing a new 400 kV line to the arc furnace facility highly unlikely in the next ten years or even in a more distant future.

D. Placement of a STATCOM device by the arc furnace

Acting upon the network to mitigate flicker problems by itself is a risky assessment. Nowadays, planned network reinforcements are few and far between and do not significantly contribute to damping flicker in the area. This is why all new arc furnaces should be connected to a node with a

large short-circuit power. Thus the arc furnace would be forced to adapt to the network and not vice-versa.

One possible solution to the existing flicker-related problems is the installation of compensation devices by the arc furnace, for example a static var compensator (SVC) and a static synchronous compensator (STATCOM). The functionality of these devices lies in their ability of fast reactive power regulation with the use of power electronics switches. Their use enables compensating the large intermittent reactive power consumption of the arc furnace. Consequently, voltage fluctuations decrease along with flicker levels across the network. The level of flicker compensation of STATCOM is somewhat higher compared to the SVC.

According to a study of reactive power compensation in the Slovenian power network [1], a STATCOM device installed by the arc furnace in Fig. 3 can attenuate flicker in node 2 to a value of $P_{it} = 0.8$.

The abovementioned value $P_{it} = 0.8$ is further used as a reference in node 2 for the calculation of flicker propagation with the current injection method. The present network in Fig. 3 is used. Results are plotted in Fig. 14.

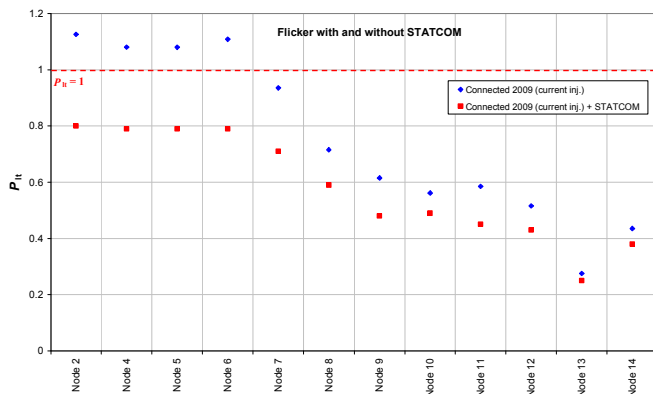


Fig. 14: Comparison of flicker values for 2009, with and without STATCOM at the arc furnace installation (both by current injection method).

The advantage in using STATCOM is evident in Fig. 14. In this case, flicker levels across the area drop below $P_{it} = 0.8$.

V. FUTURE CHANGES REGARDING FLICKER

In order to reduce electric energy consumption, the use of compact fluorescent lamps (CFLs) has been strongly promoted in recent years. This, in term, has led to a planned "phase-out" of incandescent light bulbs in several countries [12], with a ban on their sale.

The traditional definition of flicker used in [3] is however based solely on incandescent light bulbs. In the future, this definition will have to be changed in order to take CFL's and other new light sources' effect on flicker into account. This will also require a new flickermeter model with transfer functions that will cover a broader range of frequencies and not just a narrow range covered by the present model.

It is generally assumed that the replacement of incandescent light bulbs with newer light sources, which are mostly based on electronic circuit ballast, will cause less flicker annoyances.

Overall flicker levels in the network will thus be reduced.

Measurements of CFL's electrical characteristics and subsequent analysis of their future impact on power networks [12] has however shown increased number of issues regarding harmonic currents and voltages.

VI. CONCLUSION

Simulation of flicker propagation in a network is essential for studies of flicker mitigation. The load-flow based and the current injection simulation methods used in this paper have delivered good results compared to the measurements. Simulations have shown that flicker continues to be a serious power quality concern in the area until 2020, unless adequate measures are taken. A new 400 kV line feeding the arc furnace will greatly decrease flicker levels in the area but is still the least likely option when economic and other aspects are considered. Installation of STATCOM at the arc furnace facility is the simplest and most cost effective method for reducing flicker in the area and no interventions in the network are required.

VII. REFERENCES

- [1] I. Papič, B. Blažič, T. Pfajfar, M. Maksić, D. Matvoz, M. B. Kobav, "Analysis of flicker propagation in the Slovenian power system", University of Ljubljana, Faculty of electrical engineering, 2008.
- [2] B. Blažič, M. B. Kobav, T. Pfajfar, U. Kerin, D. Matvoz, K. Skok, I. Papič, "Analysis of flicker levels in the Slovenian transmission network", *Electrotechnical review* 73(5) Ljubljana, pp. 291-296, 2006.
- [3] EN 50160 standard, Voltage characteristics in public distribution networks
- [4] SIST IEC/TR 61000-3-7 Slovenian standard, EMC – Assessment of emission limit for the connection of fluctuating load installations to MV, HV and EHV power systems.
- [5] H. Renner, M. Sakulin, "Flicker propagation in meshed high voltage networks", *9th international conference on harmonics and quality of power*, vol. 3, pp. 1023-1028, Oct. 2000.
- [6] S. Perera, D. Robinson, S. Elphick, D. Geddey, N. Browne, V. Smith, V. Gosbell, "Synchronized flicker measurement for flicker transfer evaluation in power systems", *IEEE Trans. on power delivery*, vol. 21, pp. 1477-1482, July, 2006.
- [7] D. Stade, H. Schau, A. Novitskiy, "Flicker analysis in the H.V. transmission system", *10th international conference on harmonics and quality of power*, vol. 2, pp. 541-546, Oct. 2002.
- [8] M. Cybelle Simoes, S. M. Deckmann, "Flicker propagation and attenuation", *10th international conference on harmonics and quality of power*, vol. 2, pp. 644-648, 2002.
- [9] B. Novo Ramos, J. F. Manzanedo Garcia, M. Perez Donsion, "Study of flicker generation and transmission in interconnected electric grids", *10th international conference on harmonics and quality of power*, vol. 1, pp. 66-70, 2002.
- [10] B. Blažič, I. Papič, "Analysis of flicker mitigation in a utility distribution network", *Eurocon 2003*, vol. 2, pp. 292-296, Sept. 2002.
- [11] UIE WG 2: *Guide to Quality of Electrical Supply for Industrial Installations, Part 5 : Flicker and Voltage Fluctuations*, UIE, Paris, 1999.
- [12] D. Matvoz, M. Maksić, "Impact of Compact Fluorescent Lamps on the Electric Power Network", *13th international conference on harmonics and quality of power, ICHQP*, 2008.

VIII. BIOGRAPHIES

Miloš Maksić (S'07) received the B.Sc. degree in electrical engineering from the University of Ljubljana, Ljubljana, Slovenia, in 2007.

Currently he is a Researcher at the Faculty of Electrical Engineering, University of Ljubljana. His research interests include power quality and power system simulations.

Boštjan Blažič received the B.Sc., M.Sc. and Ph.D. degrees, all in electrical engineering from the University of Ljubljana, Ljubljana, Slovenia, in 2000, 2003 and 2005, respectively.

From 2000 to 2006 he worked as a researcher at the Faculty of Electrical Engineering. Currently he is as an assistant at the same faculty. Besides teaching, his work includes research in the fields of power quality, active compensators, operation of power converters and integration of distributed generation.

Igor Papič (S'97-A'99-M'00-SM'06) received the B.Sc., M.Sc. and Ph.D. degrees, all in electrical engineering, from the University of Ljubljana, Ljubljana, Slovenia in 1992, 1995 and 1998, respectively.

From 1994 to 1996, he was with Siemens Power Transmission and Distribution Group in Erlangen, Germany. Currently, he is an Associate Professor at the Faculty of Electrical Engineering, University of Ljubljana. In 2001 he was a Visiting Professor at the University of Manitoba, Winnipeg, Canada. His research interests include power quality, power system simulations, control and modeling of FACTS devices and power conditioners.